PRESSURE DROP OF THREE-PHASE SUSPENSION FLOWS (WATER–AIR–SAND) IN HORIZONTAL PIPELINES: MODEL REVISION AND GENERALIZED CORRELATION

Filippo Pironti[1]

Resumo
Os resultados experimentais e o modelo de uma única equação originalmente apresentados por Pironti et al. (1997) para o escoamento trifásico de suspensões — gás, líquido e sólido — em tubulações horizontais são revisitados à luz de quase três décadas de pesquisas subsequentes. Os gradientes de pressão foram medidos em uma tubulação horizontal com diâmetro interno de 3,5 cm e comprimento de 4,7 m, em função da velocidade da suspensão (0,5–1,3 m/s) e da velocidade superficial do ar (0–0,2 m/s), para concentrações de areia entre 5% e 40% v/v. A injeção de gás reduziu o gradiente de pressão sempre que o escoamento se encontrava segregado, com a presença de leito móvel e elevada concentração de sólidos, e o aumentou quando as partículas estavam completamente suspensas. Os quarenta pontos experimentais, recuperados neste estudo por meio da digitalização das figuras originais, são apresentados em forma tabular pela primeira vez. O modelo original foi aprimorado em três aspectos: (i) a fração volumétrica de gás sem deslizamento foi substituída por uma estimativa, baseada no modelo de fluxo de deriva, da fração de gás in situ; (ii) a velocidade de sedimentação livre em água pura foi substituída pela velocidade de sedimentação impedida de Richardson–Zaki, tornando explícita a dependência em relação à concentração de sólidos; e (iii) permitiu-se que o fator de atrito da polpa, tratada como um pseudofluido, variasse em função do número de Reynolds. Com o fator de atrito de Blasius, a inclinação prevista do gradiente de pressão adimensional em relação ao logaritmo da velocidade da suspensão torna-se $-(3 - 1/4) = -2{,}75$, valor compatível com $-2{,}79$, publicado para os dados combinados de ampla faixa de velocidades deste trabalho e de Adams et al. (1995). A recalibração com base nos dados recuperados demonstra que a constante empírica do modelo aprimorado se mantém uniforme, com variação de até 15%, ao longo de uma faixa de concentração equivalente a 4,4 vezes, enquanto a constante do modelo original varia mais de 60%. O desvio absoluto médio do gradiente de pressão total previsto diminui de 20% para 15%, e o desvio máximo, de 73% para 36%. O conjunto de dados, que abrange concentrações de sólidos muito superiores às da maioria dos estudos publicados sobre escoamentos trifásicos, é disponibilizado como base de validação para modelos mecanísticos em camadas e simulações de dinâmica dos fluidos computacional (CFD).
Palavras-chave: queda de pressão; escoamento trifásico; polpa; injeção de gás; tubulação horizontal; fluxo de deriva; sedimentação impedida.

Abstract
The experimental results and the one-equation model originally reported by Pironti et al. (1997) for three-phase (gas–liquid–solid) suspension flow in horizontal pipes is revisited in light of nearly three decades of subsequent research. Pressure gradients were measured in a 3.5 cm ID, 4.7 m long horizontal pipe as functions of the suspension velocity (0.5–1.3 m/s) and the air superficial velocity (0–0.2 m/s), for sand concentrations of 5–40% v/v. Gas injection reduced the pressure gradient whenever the flow was segregated (moving bed present, high solids concentration) and increased it when the particles were fully suspended. The forty experimental points, recovered here by digitizing the original figures, are tabulated for the first time. The original model is upgraded in three respects: (i) the no-slip gas holdup is replaced by a drift-

[1] Ph. D. pela Cornell University, Ithaca, N.Y - E.U.A; professor do Departamento de Termodinámica y Fenómenos de Transferencia da Universidad Simón Bolívar-Venezuela;. E-mail: filippo@usb.ve.

flux estimate of the in-situ gas fraction; (ii) the free-settling velocity in pure water is replaced by the Richardson–Zaki hindered-settling velocity, making the solids-concentration dependence explicit; and (iii) the friction factor of the slurry, treated as a pseudo-fluid, is allowed to vary with the Reynolds number. With a Blasius friction factor, the predicted slope of the dimensionless pressure gradient against the logarithm of the suspension velocity becomes $-(3 - 1/4) = -2.75$, consistent with the value of -2.79 published for the combined wide-velocity-range data of this work and Adams et al. (1995). Recalibration against the recovered data shows that the empirical constant of the upgraded model is uniform within 15% across the 4.4-fold concentration range, whereas that of the original model varies by more than 60%; the mean absolute deviation of the predicted total pressure gradient drops from 20% to 15% and the maximum deviation from 73% to 36%. The data set, which covers solids concentrations well above those of most published three-phase studies, is offered as a validation base for mechanistic layer models and CFD simulations.
Keywords: pressure drop; three-phase flow; slurry; gas injection; horizontal pipeline; drift flux; hindered settling.

1 INTRODUCTION

The simultaneous flow of gas, liquid and solids in horizontal pipes occurs in gas-assisted hydraulic transport of minerals, in the production of crude oil with sand, in drilling muds, in dredging, in the transport of nuclear waste slurries and in fluidized-bed catalytic systems. When the original version of this work was published (Pironti et al., 1997), the literature on horizontal gas–liquid–solid pipe flow was scarce: the survey of Sharma and Rohatgi (1992) covered the gas–liquid, liquid–solid and gas–solid binary systems without addressing three-phase flows, and the few available antecedents were the works of Scott and Rao (1971), Hatate et al. (1986), Toda et al. (1969), and the measurements of Adams et al. (1995) and Gillies et al. (1997).

The original experiments, performed in a bench-scale loop with the sand–water–air system, established a finding of direct practical interest: at fixed suspension flow rate and solids concentration, the presence of gas reduces the pressure gradient whenever the flow is segregated, i.e., when a moving bed of particles exists at the bottom of the pipe. Conversely, at low solids concentration, with the particles fully suspended, gas injection increases the pressure gradient, as expected for a conventional gas–slurry two-phase flow. This dual behavior was rationalized with a simplified one-equation model following the approach of Toda et al. (1969) for liquid–solid systems.

The field has matured considerably since. Orell (2007) developed one-dimensional hydrodynamic models for gas injection into slurry transport by coupling the two-layer model of Doron et al. (1987) with a three-phase slug-flow model, and showed theoretically that the pressure gradient can decrease upon gas injection over a solids bed. Rahman et al. (2013) proposed an improved method for applying the Lockhart–Martinelli correlation to three-phase horizontal flows, treating the slurry as a pseudo-liquid whose properties are corrected with the

SRC two-layer model (Gillies and Shook, 2000; Gillies et al., 2008). New experimental databases of three-phase pressure gradients and flow regimes have been produced (Bello et al., 2005; Sassi et al., 2020), the critical sand-deposition velocity in gas–liquid flow has been characterized (Ibarra et al., 2014; Najmi et al., 2015), and Eulerian CFD with the kinetic theory of granular flow now reproduces such systems with reasonable fidelity (Messa, Malavasi and Malavasi, 2014, and later three-phase extensions).

This paper has three objectives. First, to place the original experimental data — which cover solids concentrations of 5–40% v/v, well above the ≤10% v/v range of most three-phase studies published since — within the current state of the art, and to make the data available in tabular form by digitizing the original experimental figures. Second, to review the one-equation model critically and to upgrade it with three now-standard ingredients: a drift-flux in-situ gas fraction, the Richardson and Zaki (1954) hindered-settling velocity, and a Reynolds-number-dependent slurry friction factor. Third, to quantify the improvement: the upgraded model resolves most of the residual slope discrepancy of the original correlation and roughly halves both the concentration bias of the empirical constant and the maximum prediction error.

2 PREVIOUS WORK

2.1 Liquid–solid slurry flow

Horizontal slurry transport is governed by the competition between turbulence, which suspends the particles, and gravity, which deposits them. At low mixture velocity or high concentration, a stationary or moving bed forms; at high velocity the particles are fully suspended. The boundary between regimes is characterized by the critical deposition velocity, for which classical correlations exist (Durand and Condolios, 1952; Oroskar and Turian, 1980; Turian et al., 1987). For the pressure gradient, the reference mechanistic frameworks are the two-layer model of Doron et al. (1987), its three-layer extension (Doron and Barnea, 1993) with the corresponding flow-pattern map (Doron and Barnea, 1996), and the SRC two-layer model (Gillies and Shook, 2010; Gillies et al., 2008), which approximates the velocity and concentration distributions by step functions and adds a particle friction factor for particle–wall collisions. The three-layer approach was later extended by Ramadan et al. (2005) to solids transport in horizontal and inclined channels.

2.2 Gas–liquid–solid flow in horizontal pipes

Scott and Rao (1971) first proposed that the Lockhart–Martinelli (1949) correlation, in the simplified form of Chisholm (1967), could be adapted to three-phase flow by substituting the slurry for the liquid. Hatate et al. (1986) correlated fine-particle data with this approach, and Gillies et al. (1997) reported gas–liquid–sand measurements at low velocities, observing the interaction of the gas with the solids bed. Mao et al. (1997) measured and correlated the pressure drop of three-phase flows of simulated nuclear waste slurries in a horizontal pipe. Adams et al. (1995) and Pironti et al. (1997) reported that air injection reduces the pressure gradient of concentrated sand–water suspensions whenever segregation is present.

Orell (2005, 2007) formalized these observations: he first validated a simple model for gas–liquid slug flow in horizontal pipes, and then coupled it to the two-layer model of Doron et al. (1987) to formulate the first one-dimensional hydrodynamic models for the pressure gradient with stationary and moving beds under three-phase slug flow, as well as for fully suspended flow. His analysis showed that the pressure gradient decreases upon gas injection and increases with gas superficial velocity once the bed disappears, in qualitative agreement with the earlier experimental observations of the present work. Rahman et al. (2013) demonstrated that the modified Lockhart–Martinelli correlation with SRC-corrected pseudo-liquid properties predicts three-phase frictional gradients adequately. Sassi et al. (2020) generated a database of 134 three-phase flow conditions (air–water–polypropylene) in a 30 mm horizontal pipe, confirming the performance of the modified correlation for solids less dense than the liquid.

In parallel, the petroleum industry has studied sand transport in multiphase lines for flow assurance: Bello et al. (2005) measured particle holdup profiles in horizontal three-phase pipelines; Ibarra et al. (2014) and Najmi et al. (2015) characterized the critical sand deposition velocity in stratified and intermittent gas–liquid flow at low sand loadings; and Goharzadeh et al. (2013) visualized the effect of slug flow on sand-dune transport. Eulerian–granular CFD has been applied both to fully suspended slurries (Messa, Malin and Malavasi, 2014) and to horizontal water–air–sand and industrial tailings systems, providing local concentration and velocity fields inaccessible to one-dimensional models.

Two conclusions follow. First, the dual mechanism observed in 1997 — pressure-gradient reduction by gas injection in the segregated regime, increase in the suspended regime — has been confirmed and explained mechanistically by the later literature. Second, the ingredients that the original one-equation model treated in simplified form (gas holdup, settling velocity, friction factor) now have standard treatments of comparable algebraic complexity, allowing the model to be upgraded without sacrificing its main virtue: simplicity.

3 EXPERIMENTAL

3.1 Apparatus and procedure

The experiments used the sand–water–air system in the bench-scale loop of Figure 1. A liquid–solid suspension was prepared under mechanical agitation in a 70-litre mixing tank, at sand volume concentrations of 5–40% v/v. The suspension was pumped continuously by a positive-displacement screw pump (which eliminates the pulsations of the diaphragm pump used previously) through a horizontal pipe of 4.7 m total length and 3.5 cm internal diameter. The pipe comprises an entrance section of 3.5 m (100 diameters), sufficient to ensure developed flow, and a 1.2 m test section over which the pressure drop was measured with manometric taps. The whole loop was built in carbon steel except the test section, made of plexiglass to allow visual observation of the flow regime in a smooth pipe. The suspension flow rate was controlled through a recycle to the feed tank, and the air flow was metered with a previously calibrated rotameter. All runs were performed at ambient temperature. The sand properties are those of the previous work of Adams et al. (1995). Suspension superficial velocities covered 0.5–1.3 m/s and gas superficial velocities 0–0.2 m/s.

Figure 1 - Schematic diagram of the experimental loop.

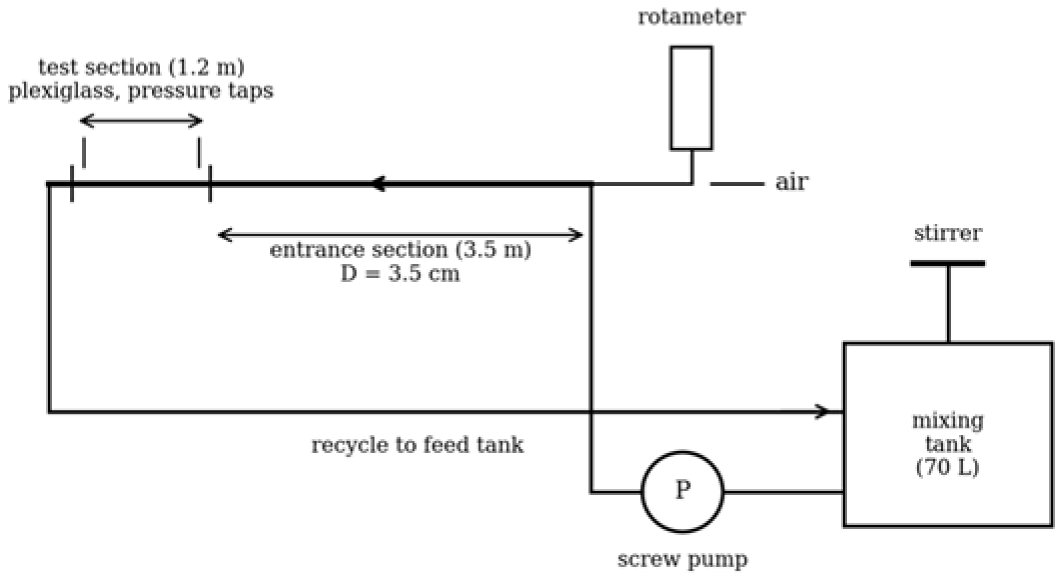

Source: Own elaboration.

3.2 Recovery of the original data

The 1997 publication reported the measurements only graphically. For the present revision the forty experimental points were recovered by semi-automatic digitization of the original figures: the markers were detected as pixel clusters, the axes were calibrated against the printed tick marks, and the series assignment was verified by cross-consistency between the two complementary representations of each data set (pressure gradient versus gas velocity and versus suspension velocity). The estimated digitization uncertainty is ±0.001–0.002 m H_2O/m, i.e. 1–2% of the measured values, smaller than the experimental scatter. Tables 1 and 2 list the recovered data; Figures 2–5 reproduce them in the format of the original paper.

Table 1 - Measured pressure gradient (m H_2O/m), C = 31.7% v/v (recovered from the original figures).

vsl (m/s)	vg = 0	vg = 0.05	vg = 0.10	vg = 0.14	vg = 0.19
0.53	0.2345	0.2118	0.1930	0.1778	0.1740
0.98	0.1969	0.1876	0.1777	0.1569	0.1513
1.13	0.1821	0.1757	0.1674	0.1608	0.1602
1.31	0.1931	0.1836	0.1708	0.1699	0.1685

Source: Own elaboration.

Table 2 - Measured pressure gradient (m H_2O/m), C = 7.2% v/v (recovered from the original figures).

vsl (m/s)	vg = 0	vg = 0.05	vg = 0.07	vg = 0.10	vg = 0.12
1.00	0.0791	0.0799	0.0807	0.0809	0.0817
1.10	0.0813	0.0875	0.0881	0.0886	0.0883
1.26	0.0833	0.0912	0.0912	0.0940	0.0969
1.30	0.0849	0.0920	0.0920	0.0955	0.0994

Source: Own elaboration.

Figure 2 - Pressure gradient versus gas superficial velocity for different suspension velocities. Average solids concentration: 31.7% v/v.

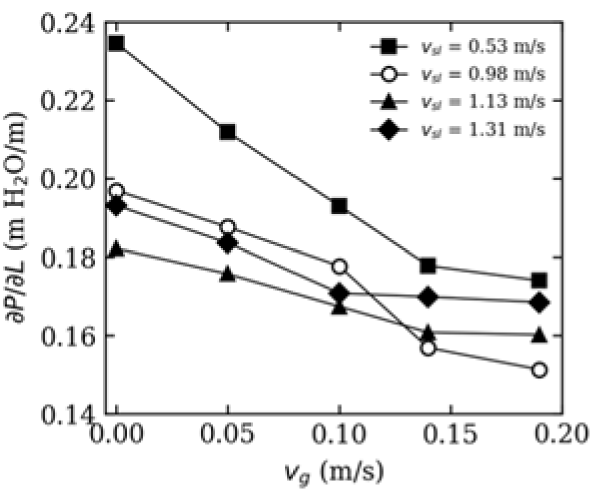

Source: Own elaboration.

Figure 3 - Pressure gradient versus suspension superficial velocity for different gas velocities. Average solids concentration: 31.7% v/v.

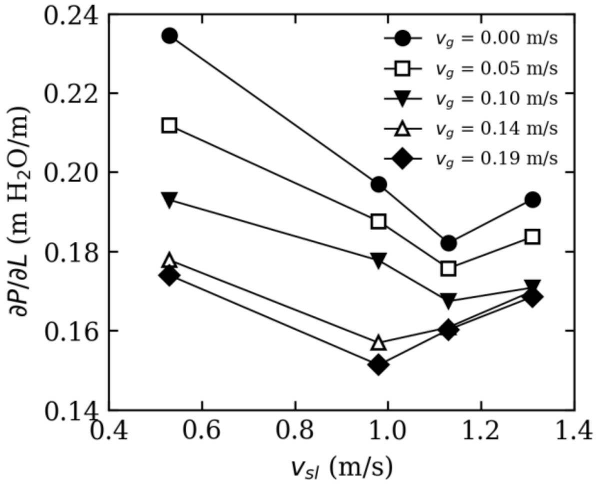

Source: Own elaboration.

Figure 4 - Pressure gradient versus gas superficial velocity for different suspension velocities. Average solids concentration: 7.2% v/v.

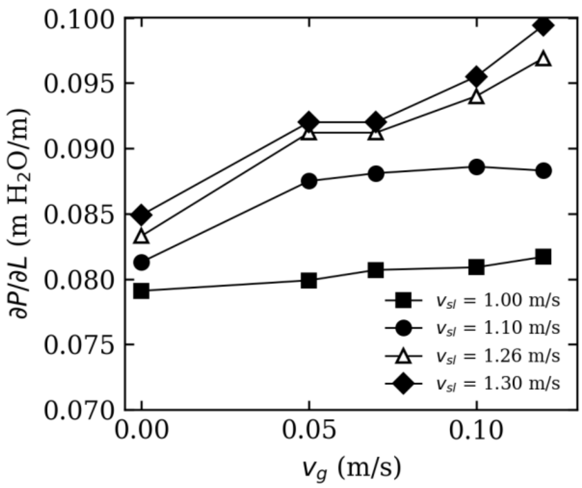

Source: Own elaboration.

Figure 5 - Pressure gradient versus suspension superficial velocity for different gas velocities. Average solids concentration: 7.2% v/v.

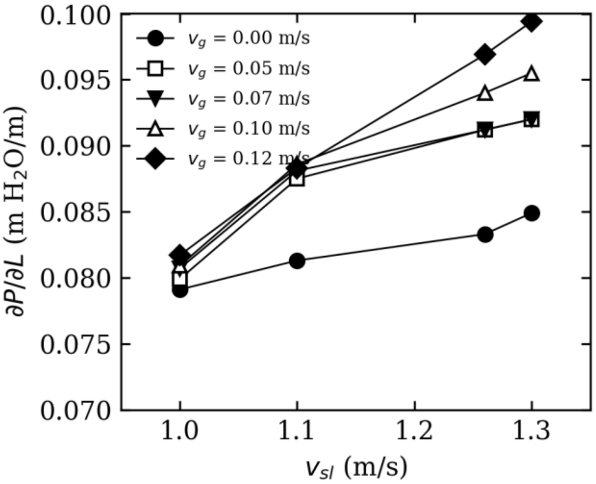

Source: Own elaboration.

4 THE ORIGINAL ONE-EQUATION MODEL

A rigorous model of horizontal three-phase flow is extremely complex; the original work adopted a simplified model following the approach of Toda et al. (1969) for liquid–solid systems. The mixture superficial velocity is

$$V_m = (Q_{sl} + Q_g)/A = v_{sl} + v_g \tag{1}$$

and, since in-situ holdups are difficult to measure, the no-slip gas holdup was used:

$$\lambda_g = Q_g \,/\, (Q_g + Q_{sl}) \tag{2}$$

The total pressure gradient was written as the sum of four contributions: (a) friction between the three-phase mixture and the pipe wall; (b) the gradient required to keep the particles in suspension; (c) friction between the moving-bed particles and the wall; and (d) friction between the gas and the liquid–solid surfaces:

$$\partial P/\partial L = \partial P_f/\partial L + \partial P_{Susp}/\partial L + \partial P_{Sf}/\partial L + \partial P_g/\partial L \tag{3}$$

Lacking correlations for the three-phase friction factor, the wall-friction term was expressed as an equivalent pressure gradient of pure water flowing at the suspension velocity, and the suspension term was postulated proportional to the free-settling velocity of the particles in pure water, $V\infty$, corrected by the slurry superficial velocity:

$$\partial P_{Susp}/\partial L = k\xi\,(1 - \lambda_g)\,C\,(\rho_s - \rho_w)\,g\cdot V\infty/V_{sl} \tag{4}$$

For full suspension (ξ = 1, no bed, wetted perimeter lw= πD), the model reduces to

$$\partial P/\partial L - (1 - \lambda_g)\,\partial P_w/\partial L = k\,(1 - \lambda_g)\,C\,(\rho_s - \rho_w)\,g\cdot V\infty/V_{sl} \tag{5}$$

and division by $C\,(1 - \lambda_g)\,\partial P_w/\partial L$ yields the dimensionless pressure gradient:

$$\Pi \equiv [\partial P/\partial L - (1 - \lambda_g)\,\partial P_w/\partial L] \,/\, [(1 - \lambda_g)\, C\partial P_w/\partial L] = 2k\,(\rho_s/\rho_w - 1)\, gDV\infty \,/\, (f \cdot V_{sl}^3) \quad (6)$$

If the friction factor f is treated as constant, Eq. (6) predicts that a plot of ln Π against ln v_{sl} is a straight line of slope −3, independent of solids concentration, gas velocity and particle size. The combined data of this work and Adams et al. (1995), spanning suspension velocities of roughly 0.14–2.7 m/s, indeed collapsed onto a straight line, but with slope −2.7856 and intercept 3.9187 ($R^2 = 0.969$):

$$\ln \Pi = 3.9187 - 2.7856 \ln v_{sl} \quad (7)$$

The deviation between the theoretical slope (−3) and the experimental one (−2.79) was left unexplained in the original work. As shown in Section 5.3, it is a direct consequence of assuming f constant.

5 IMPROVED MODEL

The additive structure of Eq. (3) and the one-equation philosophy are retained; three closures of the original model are replaced by now-standard treatments of comparable algebraic complexity.

5.1 Gas holdup with slip (drift flux)

In horizontal intermittent flow the gas travels, on average, faster than the slurry, so the in-situ gas fraction is smaller than the no-slip holdup λ_g. Following the drift-flux framework of Zuber and Findlay (1965), the in-situ gas fraction is estimated as

$$\alpha = v_g \,/\, (C_0 V_m + v_d) \quad (8)$$

where $C_0 \approx 1.2$ is the distribution parameter for intermittent flow and v_d is the drift velocity, estimated for horizontal pipes with the correlation of Bendiksen (1984):

$$v_d = 0.54\,(gD)^{1/2} \quad (9)$$

For the present conditions ($D = 0.035$ m), $v_d = 0.32$ m/s, of the same order as the gas superficial velocities employed, so the correction relative to λ_g is significant: the in-situ gas fraction is appreciably smaller than the no-slip holdup. The fraction α replaces λ_g in Eqs. (3)–(6) and in the mixture density:

$$\rho_m = (1 - \alpha)\,[\rho_w + C\,(\rho_s - \rho_w)] + \alpha\rho_g \quad (10)$$

5.2 Hindered settling

The original work acknowledged as a simplifying assumption the use of the free-settling velocity of a single particle in pure water, $V\infty$. At the concentrations studied (up to 40% v/v) the hydrodynamic interaction between particles strongly reduces the effective settling velocity. The classical correction is that of Richardson and Zaki (1954):

$$V_h = V\infty\,(1 - C)^n \tag{11}$$

where the exponent n ranges from 4.65 (Stokes regime, $Re_p < 0.2$) to 2.39 (inertial regime, $Re_p > 500$), with interpolating expressions for the intermediate regime (Rowe, 1987). For the sand of this work, taking a mean particle diameter of 0.30 mm (to be replaced by the value of Adams et al., 1995, when the tabulated properties are available), a Schiller–Naumann drag balance gives $V\infty = 43$ mm/s, $Re_p = 13$ and $n = 3.42$; hence $(1 - C)^n = 0.27$ at $C = 0.317$ and 0.77 at $C = 0.072$. Substituting V_h for $V\infty$ in Eq. (4) makes the concentration dependence of the suspension term explicit — the original model absorbed it into the empirical constant k — which, as shown in Section 6, is precisely what makes the constant uniform across concentrations.

5.3 Reynolds-number-dependent friction factor

The original model referenced wall friction to pure water flowing at the suspension velocity, with an implicitly constant friction factor. A more realistic treatment regards the slurry as a Newtonian pseudo-fluid of density $\rho_{sl} = \rho_w + C(\rho_s - \rho_w)$ and effective viscosity given, e.g., by the correlation of Thomas (1965):

$$\mu_{sl}/\mu_w = 1 + 2.5C + 10.05C^2 + 0.00273\,\exp(16.6C) \tag{12}$$

so that the slurry frictional gradient is

$$\partial P_{sl}/\partial L = f_{sl}\,\rho_{sl}V_{sl}^2\,/\,(2D) \tag{13}$$

with the friction factor evaluated from $Re_{sl} = \rho_{sl}V_{sl}D/\mu_{sl}$. In the hydraulically smooth turbulent range of the experiments ($Re_{sl} \approx 2{\times}10^4$–$5{\times}10^4$) the Blasius form is adequate:

$$f_{sl} = 0.316\,Re_{sl}^{-1/4} \tag{14}$$

This modification has an immediate, testable consequence. Substituting Eq. (14) into Eq. (6), the dimensionless gradient scales as

$$\Pi \propto V_h\,/\,(f_{sl}V_{sl}^3) \propto V_{sl}^{-(3\,-\,1/4)} = V_{sl}^{-2.75} \tag{15}$$

The theoretical log-log slope is no longer −3 but −2.75, matching the published wide-range experimental value of −2.7856 (Eq. 7) within 1.3%. The residual discrepancy of the original model is thus explained almost entirely by the Reynolds-number dependence of the friction factor, with no additional parameters. More generally, if $f_{sl} \propto Re_{sl}^{-b}$, the predicted slope is $-(3 - b)$, which also suggests a way of inferring the effective friction regime from the experimental slope.

5.4 Proposed generalized correlation

Combining the three upgrades, the fully suspended model ($\xi = 1$) reads

$$\partial P/\partial L - (1 - \alpha)\partial P_{sl}/\partial L = k'(1 - \alpha)C(\rho_s - \rho_w)g \cdot V_h/V_{sl} \quad (16)$$

with the corresponding dimensionless gradient

$$\Pi' = 2k'(\rho_s/\rho_w - 1)gDV\infty(1 - C)^n / (f_{sl}V_{sl}^3) \quad (17)$$

which can be recast in terms of a densiometric Froude number, $\mathrm{Fr} = V_{sl}/[gD(\rho_s/\rho_w - 1)]^{1/2}$, and the ratio V_h/V_{sl}, the usual grouping of modern solids-transport correlations. The constant k' is re-estimated by regression in Section 6.

5.5 Segregated regime and transition criterion

When $\xi < 1$ a moving bed exists and the four-term structure of Eq. (3) remains valid, with the bed–wall friction term of the original work. The later literature allows the model to be closed in two ways. The first is regime-predictive: the condition $\xi = 1$ is reached when the slurry velocity exceeds the critical deposition velocity, estimable with the Oroskar and Turian (1980) correlation for the gas-free case and with the correlations of Ibarra et al. (2014) and Najmi et al. (2015) in the presence of gas; this accounts for the critical velocity observed experimentally in Figure 3, beyond which the pressure gradient again grows with the suspension flow rate. The second is structural: for future work requiring more resolution than a one-equation model, the gas-augmented two-layer framework of Orell (2007) — momentum balances per layer, with a gas–slurry upper layer over a moving bed — is the natural extension, and the present data (in particular the 31.7% v/v runs with a visually confirmed moving bed) are directly usable for its validation.

The physical mechanism of the pressure-gradient reduction by gas injection in the segregated regime, observed here and in Adams et al. (1995), is consistent with this framework: the gas preferentially occupies the upper part of the cross-section, increases the in-situ velocity of the slurry layer at fixed flow rate, promotes bed erosion and reduces the effective wetted perimeter of the moving bed, so that the decrease of the first and third terms of Eq. (3) outweighs the increase of the gas term. When the concentration is low and no bed exists (7.2% v/v), the system behaves as a gas–slurry two-phase flow and the pressure gradient grows monotonically with gas flow, as predicted by the modified Lockhart–Martinelli correlation (Rahman et al., 2013) and observed by Sassi et al. (2020).

6 RESULTS AND DISCUSSION

6.1 Experimental trends

At an average solids concentration of 31.7% v/v (Figures 2 and 3, Table 1), the pressure gradient with air injection was always lower than the corresponding gas-free value, and a segregated regime with a moving bed was visually observed in most runs. At constant suspension velocity the gradient decreases upon injecting gas, and a critical velocity exists beyond which the gradient again increases with suspension flow rate — the point at which the moving bed disappears and all particles become suspended. In the framework of Section 5.5, this critical velocity is the deposition velocity of the three-phase system, and its decrease with gas flow is qualitatively consistent with the low-concentration measurements of Najmi et al. (2015). At 7.2% v/v (Figures 4 and 5, Table 2), full suspension was observed visually and the pressure gradient increased with both gas flow and suspension velocity throughout, with no critical velocity: the behavior of a conventional gas–slurry flow. The asymmetry between the two data sets is the experimental manifestation of the regime criterion ξ, and constitutes the main value of the data: few later studies span concentrations high enough to capture both sides of the transition in a single loop.

6.2 Dimensionless gradient and slope

Figure 6 shows $\ln \Pi$, computed from the recovered data with the original definition (Eq. 6, no-slip holdup, Blasius water gradient), against $\ln v_{sl}$. The forty points of both concentrations collapse onto a common band, confirming the collapse reported in 1997. The least-squares slope of the recovered subset is -2.04 ± 0.13 ($R^2 = 0.87$). This value is flatter than the published -2.7856 for two reasons that should be stated plainly: the recovered subset spans only a factor 2.5 in velocity (0.53–1.31 m/s), less than half a logarithmic decade, whereas the published fit included the Adams et al. (1995) data extending the range to roughly 0.14–2.7 m/s (a factor of about twenty); and the 31.7% points at low velocity are segregated, so part of their pressure gradient is bed friction not represented by Eq. (5), which flattens the apparent slope over a short range. Slope inference therefore requires the wide-range combined data, for which the published value of -2.7856 stands — and that value agrees within 1.3% with the -2.75 predicted by the improved model (Eq. 15), against 7% for the constant-friction value of -3. The near coincidence of the wide-range slope with the Blasius exponent also confirms a posteriori that the slurry behaved as a hydraulically smooth turbulent pseudo-fluid over the range tested.

Figure 6 - Dimensionless pressure gradient (original definition, Eq. 6) versus suspension velocity for the recovered data, with the narrow-range fit and the two theoretical slopes.

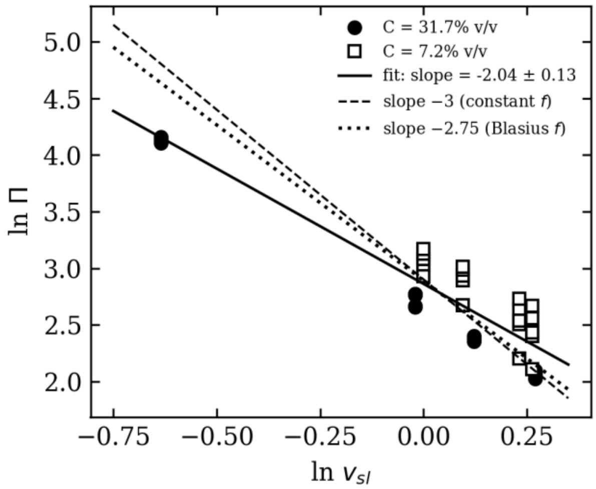

Source: Own elaboration.

6.3 Recalibration of the model constant

The most sensitive test of the upgrades is the uniformity of the empirical constant across concentrations. Solving Eq. (5) for k point by point with the original closures ($V\infty$, λ_g, water friction) gives $k = 6.7 \pm 1.0$ at $C = 31.7\%$ and $k = 10.9 \pm 1.6$ at $C = 7.2\%$: a 63% difference, i.e. the "constant" is not constant, because the hindered-settling effect it silently absorbs changes with concentration. Solving Eq. (16) for k' with the upgraded closures (V_h, α, slurry pseudo-fluid) gives $k' = 12.0 \pm 1.0$ at 31.7% and $k' = 10.4 \pm 1.6$ at 7.2%: the difference falls to 15%, within the scatter of either group, and the pooled value is $k' = 11.2 \pm 1.5$ (coefficient of variation 14%, against 29% for the original k). Figure 8 summarizes this comparison. The residual 15% offset is in the expected direction: the 31.7% group includes segregated points whose bed friction inflates the apparent suspension term.

Figure 7 shows the parity between measured and predicted total pressure gradients using the single pooled constant for each model. The upgraded model predicts the forty points with a mean absolute deviation of 15.0% and a maximum deviation of 35.6%; the original model with its pooled constant gives 20.4% and 73.1%, respectively. The improvement concentrates precisely where the original model fails: the low-velocity, high-concentration segregated points. Table 3 summarizes the comparison.

Figure 7 - Parity between measured and predicted total pressure gradients, using one pooled constant per model. Dashed lines: ±15%.

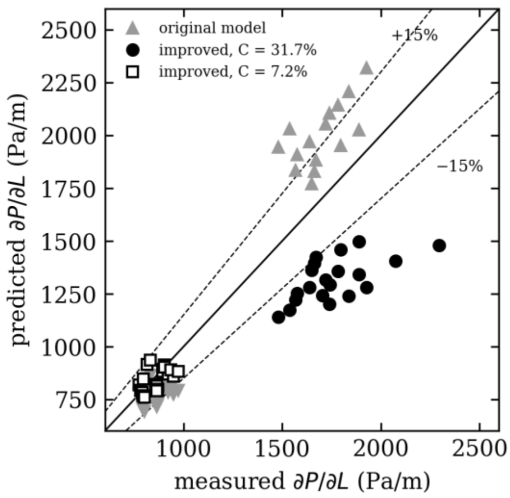

Source: Own elaboration.

Figure 8 - Model constant recalculated point by point: original k versus upgraded k′, by concentration group (error bars: one standard deviation).

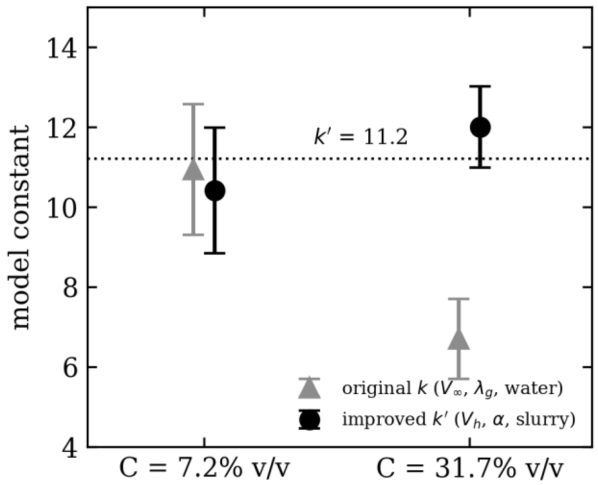

Source: Own elaboration.

Table 3 - Model comparison against the forty recovered data points.

	Original model	Improved model
Constant, C = 31.7% v/v	6.7 ± 1.0	12.0 ± 1.0
Constant, C = 7.2% v/v	10.9 ± 1.6	10.4 ± 1.6
Inter-group difference	63%	15%
Pooled CV of constant	29%	14%
Parity MAD (pooled constant)	20.4%	15.0%
Parity maximum deviation	73.1%	35.6%
Theoretical log-log slope	−3 (vs. −2.79 exp.)	−2.75 (vs. −2.79 exp.)

Source: Own elaboration.

6.4 Limitations and further validation

Three caveats apply. First, the data used here were recovered by digitizing the 1997 figures; although the estimated digitization uncertainty (1–2%) is below the experimental scatter, the original tabulated data, if located, should replace them. Second, the particle size and free-settling velocity were assumed (0.30 mm, 43 mm/s) pending the tabulated properties of Adams et al. (1995); since $V\infty$ enters k' as a scale factor, its revision changes the numerical value of k' but not the uniformity comparison, which depends on the ratio of hindered-settling factors. Third, Eq. (16) is a fully suspended model applied, for continuity with the original correlation, to all points; a two-layer treatment of the segregated points (Orell, 2007) is the natural next step and would likely remove the residual 15% offset. External validation against the open data set of Sassi et al. (2020) and the low-velocity measurements of Gillies et al. (1997), and comparison with the modified Lockhart–Martinelli method of Rahman et al. (2013), are outlined as immediate further work.

7 CONCLUSIONS

The one-equation model for the pressure gradient of air–sand–water suspension flow in horizontal pipes has been revised and upgraded, and the underlying forty-point data set — spanning solids concentrations of 7.2–31.7% v/v, a range rarely covered in the three-phase literature — has been recovered and tabulated. The experiments confirm that gas injection reduces the pressure gradient when the flow is segregated and increases it when the particles are fully suspended, a dual behaviour now explained mechanistically by gas-augmented layer models.

The upgraded model incorporates a drift-flux in-situ gas fraction, the Richardson–Zaki hindered-settling velocity and a Blasius slurry friction factor. These three ingredients, at negligible algebraic cost, (i) explain the published wide-range log-log slope of −2.79 (predicted −2.75, against −3 for constant friction); (ii) reduce the concentration bias of the empirical constant from 63% to 15% and its pooled coefficient of variation from 29% to 14%; and (iii) reduce the mean absolute deviation of the predicted total gradient from 20% to 15% and the maximum deviation from 73% to 36%. The recovered data set is offered as a validation base for mechanistic layer models and Eulerian–granular CFD of concentrated three-phase flows.

8 NOTATION

A	pipe cross-sectional area (m^2)
C	solids volume concentration in the suspension (m^3/m^3)
$C0$	drift-flux distribution parameter (-)

D	pipe internal diameter (m)
f	friction factor (-)
Fr	densiometric Froude number (-)
g	gravitational acceleration (m/s²)
k, k'	empirical constants of Equations. (4) and (16) (-)
L	length (m)
lw	wetted perimeter (m)
n	Richardson–Zaki exponent (-)
P	pressure (Pa)
Q	volumetric flow rate (m³/s)
Re	Reynolds number (-)
V, v	velocity; superficial velocity (m/s)
$V\infty$	free-settling velocity of the particles in pure water (m/s)
Vh	hindered-settling velocity (m/s)
vd	gas drift velocity (m/s)
α	in-situ gas fraction (-)
λg	no-slip gas holdup (-)
μ	dynamic viscosity (Pa·s)
ξ	fraction of suspended particles (-)
Π, Π'	dimensionless pressure gradients, Equations. (6) and (17) (-)
ρ	density (kg/m³)

Subscripts: f, friction; g, gas; m, mixture; p, particle; s, solid; sl, slurry (liquid–solid suspension); Susp, suspended; Sf, bed friction; w, water; 3-ph, three-phase.

REFERENCES

ADAMS, D.; RAMÍREZ, N.; PIRONTI, F. Transport of a three-phase slurry in horizontal pipes. In: INTERNATIONAL SCIENTIFIC-TECHNICAL CONFERENCE ON NEW METHODS AND TECHNOLOGIES IN PETROLEUM GEOLOGY, DRILLING AND RESERVOIR ENGINEERING, 6., 1995, Cracow. **Proceedings**. Cracow: [s.n.], 1995. p. 319-326.

BELLO, O. O.; REINICKE, K. M.; TEODORIU, C. Particle holdup profiles in horizontal gas–liquid–solid multiphase flow pipeline. **Chemical Engineering & Technology**, v. 28, n. 12, p. 1546-1553, 2005.

BENDIKSEN, K. H. An experimental investigation of the motion of long bubbles in inclined tubes. **International Journal of Multiphase Flow**, [s. l.], v. 10, n. 4, p. 467–483, 1984. Disponível em: https://www.sciencedirect.com/science/article/abs/pii/0301932284900570?via%3Dihub. Acesso em: 17 jul. 2026.

CHISHOLM, D. A theoretical basis for the Lockhart–Martinelli correlation for two-phase flow. **International Journal of Heat and Mass Transfer**, v. 10, p. 1767-1778, 1967. Disponível em:https://doi.org/10.1016/0017-9310(67)90047-6. Acesso em: 17 jul. 2026.

DORON, P.; GRANICA, D.; BARNEA, D. Slurry flow in horizontal pipes – experimental and modeling. **International Journal of Multiphase Flow,** v. 13, p. 535-547, 1987. Disponível em: https://doi.org/10.1016/0301-9322(87)90020-6. Acesso em: 17 jul. 2026.

DORON, P.; BARNEA, D. A three-layer model for solid-liquid flow in horizontal pipes. **International Journal of Multiphase Flow**, v. 19, n. 6, p. 1029-1043, 1993. Disponível em: https://doi.org/10.1016/0301-9322(93)90076-7. Acesso em: 17 jul. 2026.

DORON, P.; BARNEA, D. Flow pattern maps for solid-liquid flow in pipes. **International Journal of Multiphase Flow**, v. 22, p. 273-283, 1996. Disponível em: https://doi.org/10.1016/0301-9322(95)00071-2. Acesso em: 17 jul. 2026.

DURAND, R.; CONDO LIOS, E. Étude expérimentale du refoulement des matériaux en conduites. **Journées de l'hydraulique**, 2, 1952. p. 29-55. Disponível em: https://www.persee.fr/doc/jhydr_0000-0001_1953_act_2_1_3239. Acesso em: 17 jul. 2026.

GILLIES, R. G.; McKIBBEN, M. J.; SHOOK, C. A. Pipeline flow of gas, liquid and sand mixtures at low velocities. **Journal of Canadian Petroleum Technology**, v. 36, n. 9, p. 36-42, 1997. Disponível em: https://doi.org/10.2118/97-09-03. Acesso em: 17 jul. 2026.

GILLIES, R. G.; SHOOK, C. A. Modelling high concentration slurry flows. **Canadian Journal of Chemical Engineering**, v. 78, p. 709-716, 2010. Disponível em: https://doi.org/10.1002/cjce.5450780413. Acesso em: 17 jul. 2026.

GILLIES, R. G.; SHOOK, C. A.; XU, J. Modelling heterogeneous slurry flows at high velocities. **Canadian Journal of Chemical Engineering**, v. 82, p. 1060-1065, 2008. Disponível em: https://doi.org/10.1002/cjce.5450820523. Acesso em: 17 jul. 2026.

GOHARZADEH, A.; RODGERS, P.; WANG, L. Experimental characterization of slug flow on solid particle transport in a 1 deg upward inclined pipeline. **ASME Journal of Fluids Engineering**, v. 135, n. 8, p. 081304, 2013.

HATATE, Y. et al. Gas holdup and pressure drop in three-phase horizontal flows of gas – liquid – fine solid particles system. *Journal of Chemical Engineering of Japan*, v. 19, n. 4, p. 330-335, 1986. Disponível em: https://doi.org/10.1252/jcej.19.330. Acesso em: 17 jul. 2026.

IBARRA, R.; MOHAN, R. S.; SHOHAM, O. Critical sand deposition velocity in horizontal stratified flow. In: SPE INTERNATIONAL SYMPOSIUM AND EXHIBITION ON FORMATION DAMAGE CONTROL, 2014, Lafayette. **Proceedings** [...]. Lafayette: SPE, 2014. p. 1-12. (Paper SPE-168209). Disponível em: https://doi.org/10.2118/168209-MS. Acesso em: 17 jul. 2026.

LOCKHART, R. W.; MARTINELLI, R. C. Proposed correlation of data for isothermal two-phase, two-component flow in pipes. **Chemical Engineering Progress**, v. 45, n. 1, p. 39-48, 1949.

MAO, F.; DESIR, F. K.; EBADIAN, M. A. Pressure drop measurement and correlation for three-phase flow of simulated nuclear waste in a horizontal pipe. **International Journal of**

Multiphase Flow, v. 23, n. 2, p. 397-402, 1997. Disponível em: https://doi.org/10.1016/S0301-9322(96)00061-4. Acesso em: 17 jul. 2026.

MESSA, G. V.; MALAVASI, S. Numerical prediction of fully-suspended slurry flow in horizontal pipes**. Powder Technology**, v. 256, p. 61-70, 2014. Disponível em: https://doi.org/10.1016/j.powtec.2014.02.005. Acesso em: 17 jul. 2026.

NAJMI, K. *et al*. Experimental study of low concentration sand transport in wet gas flow regime in horizontal pipes. **Journal of Natural Gas Science and Engineering**, v. 24, p. 80-88, 2015. Disponível em: https://doi.org/10.1016/j.jngse.2015.03.018. Acesso em: 17 jul. 2026.

ORELL, A. Experimental validation of a simple model for gas–liquid slug flow in horizontal pipes. **Chemical Engineering Science**, v. 60, p. 1371-1381, 2005. Disponível em: https://doi.org/10.1016/j.ces.2004.09.082. Acesso em: 17 jul. 2026.

OROSKAR, A. R.; TURIAN, R. M. The critical velocity in pipeline flow of slurries. **AIChE Journal**, v. 26, n. 4, p. 550-558, 1980. Disponível em: https://doi.org/10.1002/aic.690260405. Acesso em: 17 jul. 2026.

PIRONTI, F. et al. Pressure drop of three-phase suspension flows (water-air-sand) in horizontal pipelines. **Revista Técnica de la Facultad de Ingeniería Universidad del Zulia**, v. 20, n. 2, p. 107-112, 1997. Disponível em: https://www.researchgate.net/profile/Filippo-Pironti/publication/292661723_Pressure_drop_of_three-phase_suspension_flows_water-air-sand_in_horizontal_pipelines/links/63e4c68d64252375639da056/Pressure-drop-of-three-phase-suspension-flows-water-air-sand-in-horizontal-pipelines.pdf. Acesso em: 17 jul. 2026.

RAHMAN, M. A.; ADANE, K. F.; SANDERS, R. S. An improved method for applying the Lockhart–Martinelli correlation to three-phase gas–liquid–solid horizontal pipeline flows. **Canadian Journal of Chemical Engineering**, v. 91, n. 8, p. 1372-1382, 2013. Disponível em: https://doi.org/10.1002/cjce.21843. Acesso em: 17 jul. 2026.

RAMADAN, A.; SKALLE, P.; SAASEN, A. Application of a three-layer modeling approach for solids transport in horizontal and inclined channels. **Chemical Engineering Science**, v. 60, p. 2557-2570, 2005. Disponível em: https://doi.org/10.1016/j.ces.2004.12.011. Acesso em: 17 jul. 2026.

RICHARDSON, J. F.; ZAKI, W. N. Sedimentation and fluidization: Part I. **Transactions of the Institution of Chemical Engineers**, v. 32, p. 35-53, 1954. Disponível em: https://garfield.library.upenn.edu/classics1979/A1979HZ20300001.pdf. Acesso em: 17 jul. 2026.

ROWE, P. N. A convenient empirical equation for estimation of the Richardson-Zaki exponent. **Chemical Engineering Science**, v. 42, p. 2795-2796, 1987. Disponível em: https://doi.org/10.1016/0009-2509(87)87035-5. Acesso em: 17 jul. 2026.

SASSI, P. *et al*. Experimental analysis of gas–liquid–solid three-phase flows in horizontal pipelines. **Flow, Turbulence and Combustion**, v. 105, p. 1035-1054, 2020. Disponível em: https://link.springer.com/article/10.1007/s10494-020-00141-1. Acesso em: 17 jul. 2026.

SCOTT, D. S.; RAO, P. K. Transport of solids by gas–liquid mixtures in horizontal pipes. **Canadian Journal of Chemical Engineering**, v. 49, p. 302-309, 1971. Disponível em: https://doi.org/10.1002/cjce.5450490302. Acesso em: 17 jul. 2026.

SHARMA, M. P.; ROHATGI, U. S. **Multiphase Flow in Wells and Pipelines**. New Jersey: ASME Editors, 1992.

THOMAS, D. G. Transport characteristics of suspension: VIII. A note on the viscosity of Newtonian suspensions of uniform spherical particles. **Journal of Colloid Science**, v. 20, p. 267-277, 1965. Disponível em: https://doi.org/10.1016/0095-8522(65)90016-4. Acesso em: 17 jul. 2026.

TODA, M. *et al*. Hydraulic conveying of solids through horizontal and vertical pipes. **International Chemical Engineering**, v. 9, p. 553-560, 1969.

TURIAN, R. M. et al. Estimation of the critical velocity in pipeline flow of slurries. **Powder Technology**, v. 51, p. 35-47, 1987. Disponível em: https://doi.org/10.1016/0032-5910(87)80038-4. Acesso em: 17 jul. 2026.

ZUBER, N.; FINDLAY, J. A. Average volumetric concentration in two-phase flow systems. **Journal of Heat Transfer**, v. 87, p. 453-468, 1965. Disponível em: https://doi.org/10.1115/1.3689137. Acesso em: 17 jul. 2026.